

Measurement and Prediction of the Gaussian Beam Effect in the Phase Doppler Technique

by

Lucio Araneo, Nils Damaschke, Cameron Tropea

Technische Universität Darmstadt
Fachgebiet Strömungslehre und Aerodynamik
Petersenstr. 30, 64287 Darmstadt, Germany

Abstract

Under certain circumstances, particle size measurements using a phase Doppler instrument can be erroneous due to the Gaussian beam effect, sometimes referred to as the trajectory effect. This is especially true under extenuating circumstances such as when, for cost reasons, only two detectors are being used, when the choice of detector off-axis and/or elevation angle is limited through the application, when the signal processing has only limited validation possibilities or if a particularly small measurement volume must be employed. All of these factors may be disadvantageous for measuring larger particles.

In this study the physical origins of the Gaussian beam effect are examined anew. The interpretation is based on determining for each light scattering order the position of the detection volume and their separations distances from each other. Using this information and the analysis of so called dual-burst signals, a method of estimating the maximum allowable particle size to avoid such effects is proposed. This estimation is primarily intended for users to evaluate or configure their system for a particular application.

Figure 1 illustrates a typical result in which the particle size is given for which the measured phase difference is altered less than 10° through unwanted scattering orders, as a function of detector position (symmetric detectors in elevation angle). These results and also the shift of detection volume position based on a geometrical optics analysis has been experimentally verified. The Gaussian beam effect has been systematically illustrated in the experiment using a stream of monodispersed droplets traversed through the measurement volume.

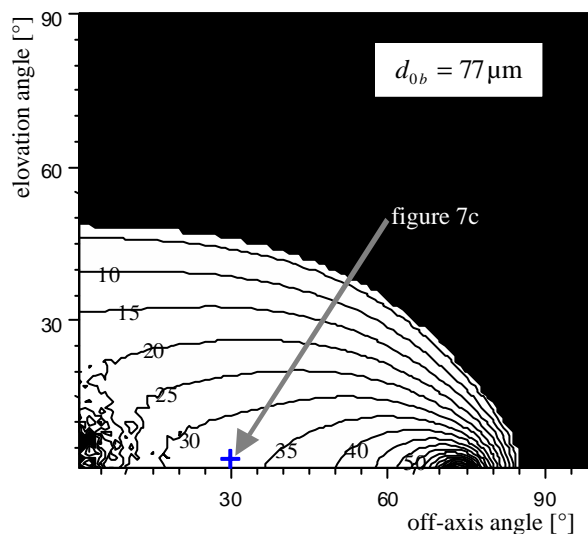


Figure 1: Particle diameter at which an error of 10° is obtained in the phase difference measurement. The laser beam diameter at the measurement volume was $77\mu\text{m}$.

1. Introduction

The phase Doppler technique is now well established as a non-intrusive method for sizing spherical, homogeneous particles and deriving corresponding volume and mass fluxes. The principle of the phase Doppler (PD) technique is based on light scattering from two plane light beams incident on the particle. The simplest PD configuration involves two detectors, placed such that a single scattering order dominates on both. Under these conditions, a linear relation between the phase difference of the detector signals and the particle diameter exists. The layout of PD systems is aided by computer programs, which compute the light scattered from spherical particles. One of the main design targets is to insure that only one scattering order dominates and for this purpose either computations according to geometrical optics [1] (for particles significantly larger than the wavelength of light) or the Lorenz-Mie theory with a Debye series expansion [2,3] can be used.

In reality however, the incident beams in a PD system cannot always be approximated by a homogeneous plane wave, especially when the particle diameter is a significant fraction of the beam waist diameter. In such cases the beam is inhomogeneous and must be treated as such in any light scattering computations. Also for scattering from inhomogeneous waves computer programs exist either based on geometrical optics [4,5], rigorous wave solutions [6] or on a Debye series expansion of the Lorenz-Mie solution [7,8]. Such simulations reveal that an inhomogeneous incident beam results in intensity variations of the scattering orders as the particle moves through the beam. Thus a photodetector at a fixed point in space will perceive a changing dominance of scattering orders from the same particle. This well known effect is the cause of the Gaussian beam effect [9]/defect [10 and references therein], sometimes referred to as the trajectory effect, and can lead to serious sizing errors. A proper simulation of the effect is time consuming and general rules of thumbs recommend applying standard phase Doppler techniques only up to particle diameters which do not exceed 1/3 or 1/2 the beam waist diameter. The Gaussian beam effect has been analysed previously and several methods for its recognition, elimination or minimisation [10,11,12,13] have been suggested. Nevertheless a reliable means of prescribing which particle size will lead to a given error level has not been provided and this is the main subject of the present contribution.

2. Measurement volumes and detection volumes

In the laser Doppler and phase Doppler techniques, laser beams with a Gaussian intensity profile are generally used. A laser beam propagating in the z direction and polarised in the y direction can be expressed as

$$\underline{E}_{yb} = \underline{E}_{0b} \frac{r_{0b}}{r_{mb}(z)} \exp\left(-\frac{x^2 + y^2}{r_{mb}(z)^2}\right) \exp\left(j\left(\omega t - k\left(z - \frac{x^2 + y^2}{2R_b(z)}\right) + \arctan\frac{z}{z_{0b}}\right)\right) \quad (1)$$

Here \underline{E}_{0b} is the field strength in the centre of the beam waist, r_{0b} is the beam waist radius, $r_{mb}(z)$ is the local beam radius, ω is the angular frequency, k the wavenumber ($2\pi/\lambda$), $R_b(z)$ is the local wave front curvature and z_{0b} is the Rayleigh length. Two such laser beams which intersect with an angle Θ form an *illuminated volume*, which is defined by the e^{-2} intensity level of the modulated part with respect to the maximum intensity and takes the shape of an ellipsoid. Very small particles effectively sample the local intensity as they pass through the volume. The incident and glare points basically all lie together on the particle surface due to its small dimensions. The limits of the *detection volume* depend on the scattered light intensity, on the photodetector location and specifications, on the signal characteristics, the signal detection criteria, possibly on the number of signal periods, etc. The detection volume is thus the volume within which the sum of all scattering order intensities results in a received signal amplitude exceeding the detection threshold and therefore may be larger or smaller than the illuminated volume. The detection threshold may be solely based on amplitude or, as in several newer processors, be sensitive to a given signal-to-noise ratio being exceeded.

For larger particles the separation between the incident points on the surface of the particle and the centre of the particle can no longer be neglected. As the particle moves through the measurement volume its surface samples the local intensity profile of the beam. The interference of the two beams now takes place in the scattered field as the interference of the two scattered waves. Since the geometric path of the light through the particle is dependent on the scattering order, each scattering order has two incident points corresponding to each of the beams. Each pair of incident points results in an interference fringe system in space. Since the incident points for each scattering order are at different locations on the particle surface, a different light intensity is sampled by each. Thus each scattering order has its own *measurement volume*. These volumes are each defined in extent by the e^{-2} decay from the point of its maximum intensity. Thus they are the same size and shape as the illuminated volume, despite the fact that they may be displaced and exhibit different absolute intensities.

The displacement of the volume for scattering order N can be in all three coordinate directions. Given the position of the two incident points for each of the beams on the particle surface (with respect to the centre of the particle of radius r_p) [5]

$$\text{Beam 1: } \mathbf{e}_1^{(N)} = r_p \begin{bmatrix} e_{1x}^{(N)} \\ e_{1y}^{(N)} \\ e_{1z}^{(N)} \end{bmatrix} \quad \text{Beam 2: } \mathbf{e}_2^{(N)} = r_p \begin{bmatrix} e_{2x}^{(N)} \\ e_{2y}^{(N)} \\ e_{2z}^{(N)} \end{bmatrix} \quad (2)$$

the position of maximum intensity and the centre of the measurement volume for scattering order N is given by [5]

$$\mathbf{r}_{max}^{(N)} = \begin{bmatrix} x_{max}^{(N)} \\ y_{max}^{(N)} \\ z_{max}^{(N)} \end{bmatrix} = -\frac{r_p}{2} \begin{bmatrix} (e_{1x}^{(N)} + e_{2x}^{(N)}) - (e_{1z}^{(N)} - e_{2z}^{(N)}) \tan \theta/2 \\ e_{1y}^{(N)} + e_{2y}^{(N)} \\ (-e_{1x}^{(N)} + e_{2x}^{(N)}) \cot \theta/2 + (e_{1z}^{(N)} + e_{2z}^{(N)}) \end{bmatrix} \quad (3)$$

where the origin of $\mathbf{r}_{max}^{(N)}$ is the centre of the illuminated volume. Each measurement volume also exhibits a detection volume, as defined above and the displacement position of the measurement and detection volumes depends linearly on particle size. This separation is shown schematically in figure 2.

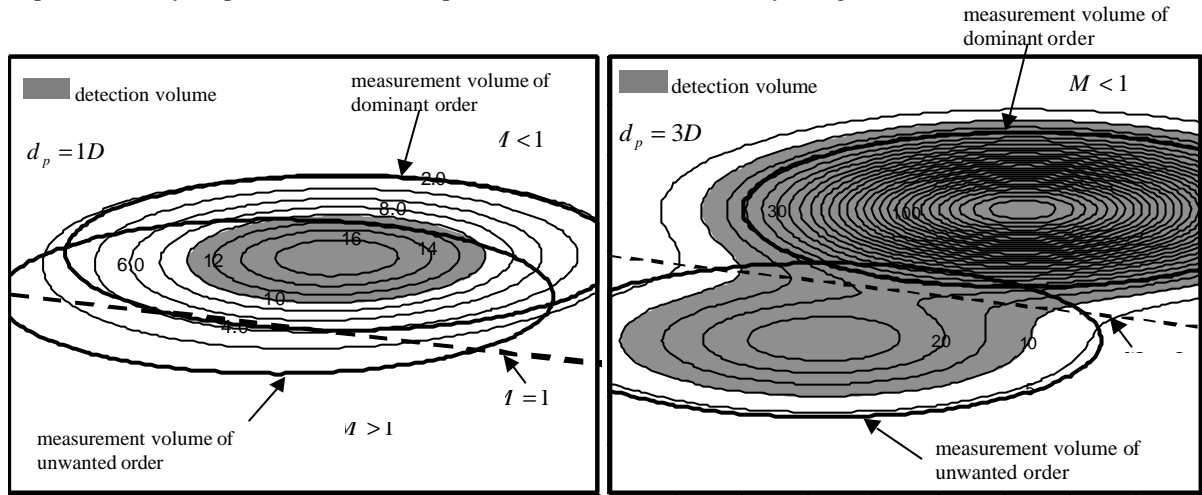


Figure 2: Schematic representation of the total scattered intensity (—), the measurement volumes ($\hat{\mathbf{A}}$), the detection volume (γ) and the amplitude ratio $M = 1$ (- - -) of the unwanted to dominant scattering order intensity for two different particle diameters.

With increasing particle size this separation leads to a change of scattering order dominance within the generated signal. In such a case erroneous phase Doppler measurements can result. This is generally known as the Gaussian beam effect, also sketched in figure 3 and figure 4.

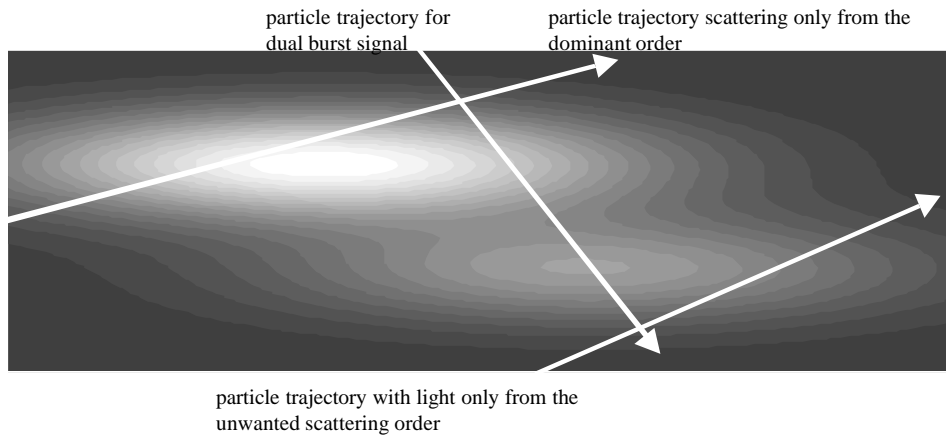


Figure 3: Scattering intensity distribution summed over all scattering orders.

In fact, the amplitude ratio between scattered intensity from the unwanted scattering order to that from the intended scattering order (M) changes throughout all space. For an infinitely sensitive detector, trajectories exist for which particles of any size will be improperly evaluated. In practice however, this only occurs when the trajectories fall within the generally complex shaped detection volume. If errors occur for an amplitude ratio of unwanted to dominant scattering order M exceeding $M = 1$, then figure 1 indicates that this is not the case for a particle of diameter $d_p = 1D$, because the detection volume lies completely in the half plane where one scattering order is dominant, whereas for $d_p = 3D$ the detection volume includes such regions of high amplitude ratio $M > 1$.

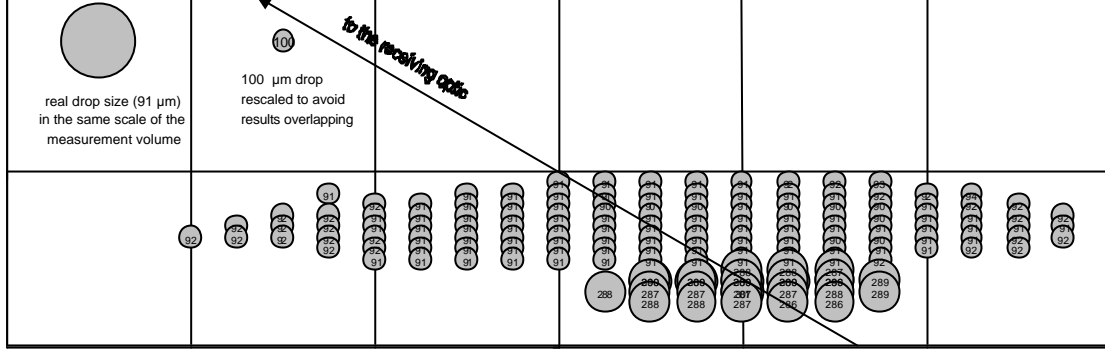


Figure 4: Measurements of 91 μm water droplets moving through the detection volumes of two different scattering orders and processed with refraction mode assumption. The direction of the particle trajectory is perpendicular to the pictured plane.

In the following analysis, particle trajectories for which measurement errors occur are to be found. The criteria used is the phase error which occurs and the amplitude of the modulation part of the signal, which must exceed some minimum detection level.

3. Dual Bursts

For this analysis the form of the signal generated at the detector is given by a dual burst expression

$$B(t) = A \left[\exp \left(- \left(\frac{t - t^{(d)}}{w} \right)^2 \right) \cos(\omega_b t + \varphi^{(d)}) + M \exp \left(- \left(\frac{t - t^{(u)}}{w} \right)^2 \right) \cos(\omega_b t + \varphi^{(u)}) \right] \quad (4)$$

whereby A is the signal amplitude of the dominating order, t is time, w is the burst width, ω_b is the burst frequency, $t^{(d)}$ and $t^{(u)}$ are the size dependent time shifts of the two bursts from each scattering order ($^{(d)}$ -dominant, $^{(u)}$ -unwanted), $\varphi^{(d)}$ and $\varphi^{(u)}$ are the size dependent signal phases from the two scattering orders and M is the amplitude ratio of the unwanted to dominant scattering order intensity ($M < 1$ for plane wave case). A phase Doppler system would determine from such a signal using e.g. a Fourier transform, the signal phase at the frequency $\omega = \omega_b$

$$\phi(\omega = \omega_b) = \arctan \frac{\sin \varphi^{(d)} + M \sin \varphi^{(u)}}{\cos \varphi^{(d)} + M \cos \varphi^{(u)}} \quad (5)$$

given sufficient periods in the signal ($\omega_b > 30/w$). It is important to note that the detection volume displacement and thus the time shift of the signal always exists. The Fourier transform of equation (4) gives a time shift dependent spectrum. Only at the burst frequency $\omega = \omega_b$ is this dependency cancelled and the result corresponds to the results from Qui et. al [12]. By using the phase factors between phase difference and particle diameter of the dominating ($C^{(d)}$) and unwanted scattering order ($C^{(u)}$) one obtain

$$\phi(\omega = \omega_b) = \arctan \frac{\sin(d_p C^{(d)}) + M \sin(d_p C^{(u)})}{\cos(d_p C^{(d)}) + M \cos(d_p C^{(u)})} \quad (6)$$

and only the two parameters d_p and M are unknown. By using a second independent phase Doppler measurement of the same particle it is possible to determine the particle diameter and the ratio between unwanted to dominant scattering order M from the two equations. These is the technique of Qiu et. al [12] to eliminate the Gaussian beam effect.

If the linear relation between particle diameter d_p and phase is substituted for each scattering order, $\varphi^{(d)} = C^{(d)}d_p$ and $\varphi^{(u)} = C^{(u)}d_p$, the absolute error can be expressed as

$$\sigma = \phi(\omega = \omega_b) - \varphi^{(d)} = \left| \arctan \frac{M \sin(d_p (C^{(u)} - C^{(d)}))}{1 + M \cos(d_p (C^{(u)} - C^{(d)}))} \right| \quad (7)$$

If for instance first order refraction is dominating, $C^{(d)} = C^{(1)}$, and the unwanted scattering order is reflection, $C^{(u)} = C^{(0)}$, the phase factors read

$$C^{(0)} = k \frac{\sin \varphi_2 \sin \mathbf{y}_r}{\sqrt{2(1 - \cos \varphi_2 \cos \mathbf{y}_r \cos \varphi_r)}} \quad (8)$$

$$C^{(1)} = -k \frac{m \sin \varphi_2 \sin \mathbf{y}_r}{2(1 + \cos \varphi_2 \cos \mathbf{y}_r \cos \varphi_r)(1 + m^2 - m\sqrt{2(1 - \cos \varphi_2 \cos \mathbf{y}_r \cos \varphi_r)})} \quad (9)$$

where m is the relative refractive index, φ_r is the elevation angle and φ_r is the off-axis angle of the detectors. In this case the phase error $\sigma = \phi - \varphi^{(d)}$ disappears for certain particle sizes (known as nodal points).

$$d_p = \frac{k\mathbf{p}}{C^{(u)} - C^{(d)}} \quad \begin{array}{ll} k = 0, 1, 2, \dots & \text{for } C^{(u)} - C^{(d)} > 0 \\ k = 0, -1, -2, \dots & \text{for } C^{(u)} - C^{(d)} < 0 \end{array} \quad (10)$$

Furthermore the error depends strongly on the amplitude ratio M . A useful quantity is the critical amplitude ratio at which an error of magnitude σ ($0 \leq \sigma < \pi/2$) occurs

$$M_{crit} = \left| \frac{\tan \sigma}{\left| \sin(d_p (C^{(u)} - C^{(d)})) \right| - \tan \sigma \cos(d_p (C^{(u)} - C^{(d)}))} \right| \quad (11)$$

The phase factors $C^{(d)}$ and $C^{(u)}$ are generally so large, that this critical amplitude ratio varies strongly with particle diameter. For this reason it is advantageous to define a minimum critical amplitude ratio, which is particle size independent

$$M_{crit} \left| \frac{dM_{crit}}{dd_p} \right| = \sin \sigma \quad (12)$$

4. Worst Case Particle Position

Equation (12) yields, for given phase error, detector position and particle size, an amplitude ratio of unwanted to dominant scattering order intensity which must not be exceeded to avoid errors. For plane waves this ratio would never be exceeded. For inhomogeneous beams however, trajectories will always exist for which the ratio will be exceeded (see figure 2). Of particular interest is to find the particle position \mathbf{p}_{crit} at which the ratio is exceeded and also the intensity takes a maximum. It can be shown that this position always lies on the line connecting the centres of the two detection volumes, as shown in figure 5.

The connecting line between centres \mathbf{g}_{cl} in parametric form is given from equation (3) as

$$\mathbf{g}_{cl} = \mathbf{e}_{cl} P \quad \mathbf{e}_{cl} = \begin{bmatrix} x_{cl} \\ y_{cl} \\ z_{cl} \end{bmatrix} = \frac{\mathbf{r}_{max}^{(d)} - \mathbf{r}_{max}^{(u)}}{\left| \mathbf{r}_{max}^{(d)} - \mathbf{r}_{max}^{(u)} \right|} \quad (13)$$

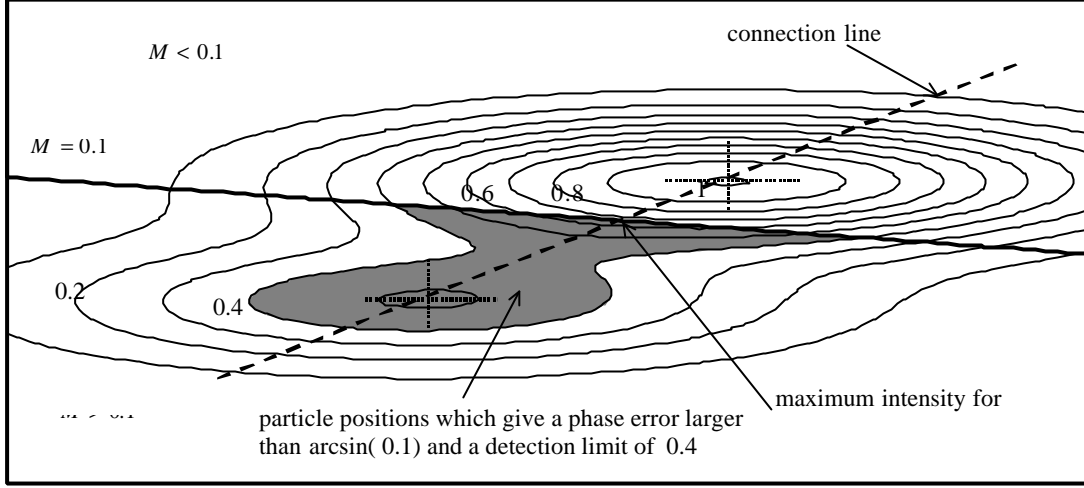


Figure 5: Relation between the detection volume centres and the position of maximum signal intensity at which a given amplitude ratio is exceeded.

p is here the position parameter along the line. The ratio of unwanted (u) to dominating (d) scattering order intensity can be written as,

$$M(\mathbf{g}_{cl}) = M_0 \frac{\exp\left(-\frac{1}{r_m^2} \left((x_{cl}p + e_{1x}^{(u)}r_p)\cos\frac{\Theta}{2} - (z_{cl}p + e_{1z}^{(u)}r_p)\sin\frac{\Theta}{2} \right)^2 + (y_{cl}p + e_{1y}^{(u)}r_p)^2 + \left((x_{cl}p + e_{2x}^{(u)}r_p)\cos\frac{\Theta}{2} + (z_{cl}p + e_{2z}^{(u)}r_p)\sin\frac{\Theta}{2} \right)^2 + (y_{cl}p + e_{2y}^{(u)}r_p)^2 \right)}{\exp\left(-\frac{1}{r_m^2} \left((x_{cl}p + e_{1x}^{(d)}r_p)\cos\frac{\Theta}{2} - (z_{cl}p + e_{1z}^{(d)}r_p)\sin\frac{\Theta}{2} \right)^2 + (y_{cl}p + e_{1y}^{(d)}r_p)^2 + \left((x_{cl}p + e_{2x}^{(d)}r_p)\cos\frac{\Theta}{2} + (z_{cl}p + e_{2z}^{(d)}r_p)\sin\frac{\Theta}{2} \right)^2 + (y_{cl}p + e_{2y}^{(d)}r_p)^2 \right)} \quad (14)$$

whereby the laser beam radius r_m in the vicinity of the measurement volume can be considered constant. M_0 is the amplitude ratio for plane waves, r_p is the particle radius, Θ is the full intersection angle of the beams and $e_{1,2,x,y,z}^{(u,d)}$ are the coordinates of the incident points for laser beams 1 and 2 from equation (2) for each scattering order.

This equation allows the position along the connecting line to be re-formulated as a function of p . The particle position $\mathbf{p} = \mathbf{e}_{cl}p$ depends on particle diameter $d_p = 2r_p$, the selected amplitude ratio M , the ratio for plane waves M_0 and the geometric configuration of the phase Doppler system.

$$\mathbf{p}(r_p, \Phi_r, \Psi_r, M, M_0) = \mathbf{e}_{cl} \frac{1}{2A} \left(Br_p + \ln\left(\frac{M}{M_0}\right) \frac{r_m^2}{r_p} \right) \quad (15)$$

with

$$B = (E_z - E_x)\cos^2\frac{\Theta}{2} - 2F\sin\frac{\Theta}{2}\cos\frac{\Theta}{2} - (E_z + E_y) \quad (16)$$

$$A = (C_x x_{cl} - C_z z_{cl})\cos^2\frac{\Theta}{2} + (D_x z_{cl} + D_z x_{cl})\sin\frac{\Theta}{2}\cos\frac{\Theta}{2} + C_y y_{cl} + C_z z_{cl} \quad (17)$$

and

$$C = \begin{bmatrix} C_x \\ C_y \\ C_z \end{bmatrix} = \mathbf{e}_1^{(d)} + \mathbf{e}_2^{(d)} - (\mathbf{e}_1^{(u)} + \mathbf{e}_2^{(u)}), \quad D = \begin{bmatrix} D_x \\ D_y \\ D_z \end{bmatrix} = \mathbf{e}_1^{(u)} - \mathbf{e}_2^{(u)} - \mathbf{e}_1^{(d)} + \mathbf{e}_2^{(d)} \quad (18)$$

$$E = \begin{bmatrix} E_x \\ E_y \\ E_z \end{bmatrix} = \begin{bmatrix} (e_{1x}^{(d)})^2 + (e_{2x}^{(d)})^2 - (e_{1x}^{(u)})^2 - (e_{2x}^{(u)})^2 \\ (e_{1y}^{(d)})^2 + (e_{2y}^{(d)})^2 - (e_{1y}^{(u)})^2 - (e_{2y}^{(u)})^2 \\ (e_{1z}^{(d)})^2 + (e_{2z}^{(d)})^2 - (e_{1z}^{(u)})^2 - (e_{2z}^{(u)})^2 \end{bmatrix}, \quad F = e_{1x}^{(u)}e_{1z}^{(u)} - e_{2x}^{(u)}e_{2z}^{(u)} - e_{1x}^{(d)}e_{1z}^{(d)} + e_{2x}^{(d)}e_{2z}^{(d)} \quad (19)$$

For M in equation (15), the critical amplitude ratio M_{crit} from equations (11) or (12) can be substituted. Thus an analytic expression results which gives the exact position $\mathbf{p}_{crit} = \mathbf{e}_{cl} p_{crit}$ at which a prescribed error occurs while the signal exhibits a maximum intensity

$$\mathbf{p}_{crit} = \begin{bmatrix} p_x \\ p_y \\ p_z \end{bmatrix} = \mathbf{e}_{cl} \frac{1}{2A} \left(B \frac{d_p}{2} + 2 \frac{r_m^2}{d_p} \ln \left(\frac{\tan \sigma}{M_0 \left| \left| \sin(d_p (C^{(u)} - C^{(d)})) \right| - \tan \sigma \cos(d_p (C^{(u)} - C^{(d)})) \right|} \right) \right) \quad (20)$$

The phase factors $C^{(d)}$ and $C^{(u)}$ are found from the geometry of the phase Doppler system, e.g. equations (8) and (9) for reflection and refraction.

Along the connecting line between detection volume centres all amplitude ratios between $-\infty$ and $+\infty$ occur, arising from the superposition of two displaced Gaussian fields. For infinitely sensitive detectors, a particle position can therefore always be found for which an error will occur. Accordingly, some further criterion must be prescribed on which the selection of error free particle sizes can be made.

An error can only occur when the scattered light intensity, being the sum of e.g. reflection and refraction, exceeds the detection level and thus the particle trajectory passes through the detection volume. Using the critical particle position $\mathbf{p}_{crit}(r_p)$, the scattering intensity of the dominating scattering order, e.g. refraction from equation (1)

$$I^{(d)}(r_p) = I_0^{(d)} \frac{r_p^2}{r_{p0}^2} \exp \left(- \frac{1}{r_m^2} \left(\left((p_x(r_p) + e_{1x}^{(d)} r_p) \cos \vartheta/2 - (p_z(r_p) + e_{1z}^{(d)} r_p) \sin \vartheta/2 \right)^2 + (p_y(r_p) + e_{1y}^{(d)} r_p)^2 + \left((p_x(r_p) + e_{2x}^{(d)} r_p) \cos \vartheta/2 + (p_z(r_p) + e_{2z}^{(d)} r_p) \sin \vartheta/2 \right)^2 + (p_y(r_p) + e_{2y}^{(d)} r_p)^2 \right) \right) \quad (21)$$

and the unwanted order, e.g. reflection

$$I^{(u)}(r_p) = I_0^{(u)} \frac{r_p^2}{r_{p0}^2} \exp \left(- \frac{1}{r_m^2} \left(\left((p_x(r_p) + e_{1x}^{(u)} r_p) \cos \vartheta/2 - (p_z(r_p) + e_{1z}^{(u)} r_p) \sin \vartheta/2 \right)^2 + (p_y(r_p) + e_{1y}^{(u)} r_p)^2 + \left((p_x(r_p) + e_{2x}^{(u)} r_p) \cos \vartheta/2 + (p_z(r_p) + e_{2z}^{(u)} r_p) \sin \vartheta/2 \right)^2 + (p_y(r_p) + e_{2y}^{(u)} r_p)^2 \right) \right) \quad (22)$$

can be computed.

The maximum intensity of the individual orders

$$I_0^{(d)} \frac{r_p^2}{r_{p0}^2} \quad \text{and} \quad I_0^{(u)} \frac{r_p^2}{r_{p0}^2} \quad (23)$$

are with respect to a reference particle radius r_{p0} . To determine the ratio of the scattering order intensities given in equation (15)

$$M_0 = \frac{I_0^{(u)}}{I_0^{(d)}} \quad (24)$$

for arbitrary particle diameters, a particle size $d_{p0} = 2r_{p0}$ which is definitely large enough to be treated using geometrical optics (e.g. $d_{p0} = 100\mu\text{m}$) is considered. The scattering intensities $I_0^{(u)}$ and $I_0^{(d)}$ are determined for the case of a plane wave. The intensity increases with the square of particle size in the geometrical optics range, which will yield the maximum intensities used in equation (23) or in equations (21 and 22). If the total scattered intensity exceeds the detection amplitude

$$I = I^{(d)}(r_p) + I^{(u)}(r_p) > I_{Detection} \quad (25)$$

then erroneous measurements can be expected. The detection level $I_{Detection}$ of the detectors can be chosen such that particles with a diameter $d_{pl} = 2r_{pl} = 2\mu\text{m}$ will just be detected. The detection level can then be determined with respect to the reference particle radius.

$$I_{Detection} = \frac{r_{pl}^2}{r_{p0}^2} (I_0^{(d)}(r_p) + I_0^{(u)}(r_p)) = \frac{(0.5\mu\text{m})^2}{(50\mu\text{m})^2} (I_0^{(d)}(r_p) + I_0^{(u)}(r_p)) \quad (26)$$

The numerical solution of equation (25) for r_p yields the maximum error free particle size for the chosen detector positions. This analysis therefore provides the particle size at which first errors due to the Gaussian beam effect can be expected.

The above analysis was carried through assuming only two scattering orders interacting in the ratio M to yield the detected intensity. Indeed, the sum of all scattering orders must be considered for a more exact solution, however in most practical circumstances, off-axis and elevation angles are chosen for the detectors at which higher order scattering is negligibly small. Furthermore, the relatively simple expressions given above would no longer be possible.

5. Examples and Measurements

To verify the above analysis a number of measurements were performed using a conventional three detector phase Doppler receiver from the company DANTEC. The three detectors allows in principle measurements of particles which result in phase differences exceeding 360° . If the three detectors are also non-symmetric in elevation angle and the ratio of the phase factors of the two detector pairs is not an integer (best value: 1.5, 2.5, 3.5,...), they can identify the Gaussian beam effect to some extent, as illustrated in figure 6a. If a symmetrical arrangement of apertures is used (for instance when small particles are being measured), or when the ratio of the phase factors is an integer value, then the Gaussian beam effect can no longer be identified using the three detector arrangement (figure 6b). However even for asymmetric arrangements, an error free result is not always possible, especially when the phase difference exhibits large scatter (figure 6c). Generally the detector aperture positions in PD receiving unit are defined by the mask used in front of the receiving lens. The Dantec mask A is symmetric and therefore not recommended in situations where the Gaussian beam effect can potentially occur.

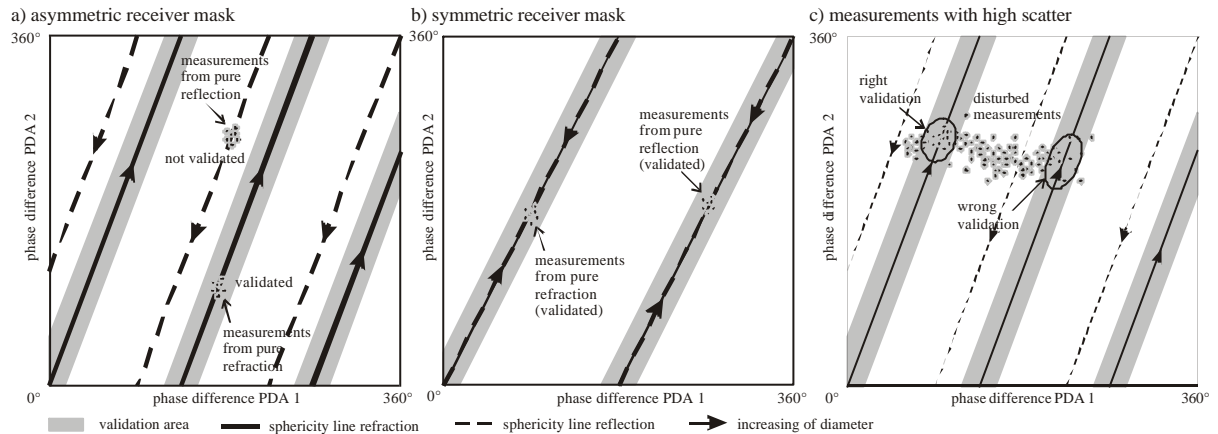


Figure 6: Identification (a) and non-identification (b,c) of the Gaussian beam effect using a conventional three detector phase Doppler receiver.

The first set of measurements was performed by scanning a polystyrol particle affixed to a needle through the measurement volume. The theoretical prediction about the position and extent of the detection volumes for each scattering order (in this case refraction (1) and reflection (0)) could be experimentally verified, as summarised in tables 1 and 2.

The deviations of detection volume centres between geometrical optics and FLMT computations can be explained by the intensity fluctuations found in the scattering lobes for small variations of scattering angle.

A second set of measurements was performed using a monodispersed stream of droplets ($d_p = 91\mu\text{m}$), traversed throughout the illuminated volume. Various configurations of the phase Doppler system were used, as summarised in table 3.

Three typical measurement results for three laser beam waist diameters ($290\mu\text{m}$, $150\mu\text{m}$, $77\mu\text{m}$) are shown in figure 7. The use of the asymmetric mask B allows reflection from refraction to be distinguished. The raw phase data were saved and then processed a first time with the refraction coefficient and validation criteria (white drops) and a second time for reflection (grey drops). In figure 7a no Gaussian beam effect is observed, i.e. no scattering due to reflection is detected. The droplet size was correctly measured throughout the entire detection volume. In contrast, the detection volume of reflection and the errors due to reflected scattered light are clearly recognised in figure 7b and figure 7c.

By increasing the particle size relative to the diameter of the illuminated volume the reflection mode becomes stronger and the detection volumes of the scattering orders are more separated. The displacement of the measurement volumes are the same in all three measurements because the same particle size is used. Also the shape of the slit located in front of the detectors is clear to see in all three measurements.

displacement of detection volume [μm]	geometrical optics	Fourier-Lorenz-Mie-Theory	Measurements
$x_{max}^{(1)}$	24.01	27 ± 0.5	-
$y_{max}^{(1)}$	77.44	86.5 ± 0.5	-
$z_{max}^{(1)}$	131.37	141 ± 3	-
$x_{max}^{(0)}$	-38.17	-38 ± 1	-
$y_{max}^{(0)}$	-129.06	-129 ± 1	-
$z_{max}^{(0)}$	-195.39	-195 ± 3	-
$2x_{max}^{(1)}$	48.02	54 ± 1	53.7 ± 0.5
$2x_{max}^{(0)}$	-76.34	-76 ± 2	-79.5 ± 0.5
$y_{max}^{(1)} - y_{max}^{(0)}$	206.50	215 ± 1.5	217 ± 5
$z_{max}^{(1)} - z_{max}^{(0)}$	326.76	336 ± 6	344 ± 5

Table 1: Comparison between computed and measured position of the detection volume centers for reflection and refraction.

dimensions of volumes	illuminated volume	refraction volume		reflection volume	
		receiver 1	receiver 2	receiver 1	receiver 2
Δx [μm]	29.2	30 ± 1	29 ± 1	30 ± 1	31 ± 1
Δy [μm]	29	32 ± 3	31 ± 2	-	-
Δz [μm]	243.1	244 ± 8	248 ± 8	248 ± 6	245 ± 7

Table 2: Comparison between computed and measurement extent of the detection volume extent for reflection and refraction.

beam separation [mm]	transmitter focal length [mm]	full beam intersection angle [°]	beam waist diameter [μm]	receiver off-axis angle [°]	receiver mask [14]
58	310	10.7	77	$\pm 30^\circ$	B, C
58	310	10.7	77	46°	B
60	310	11.1	150	$\pm 30^\circ$	B, C
60	600	5.72	290	$\pm 30^\circ$	A, B, C

Table 3.: Used configurations of the DANTEC phase Doppler system

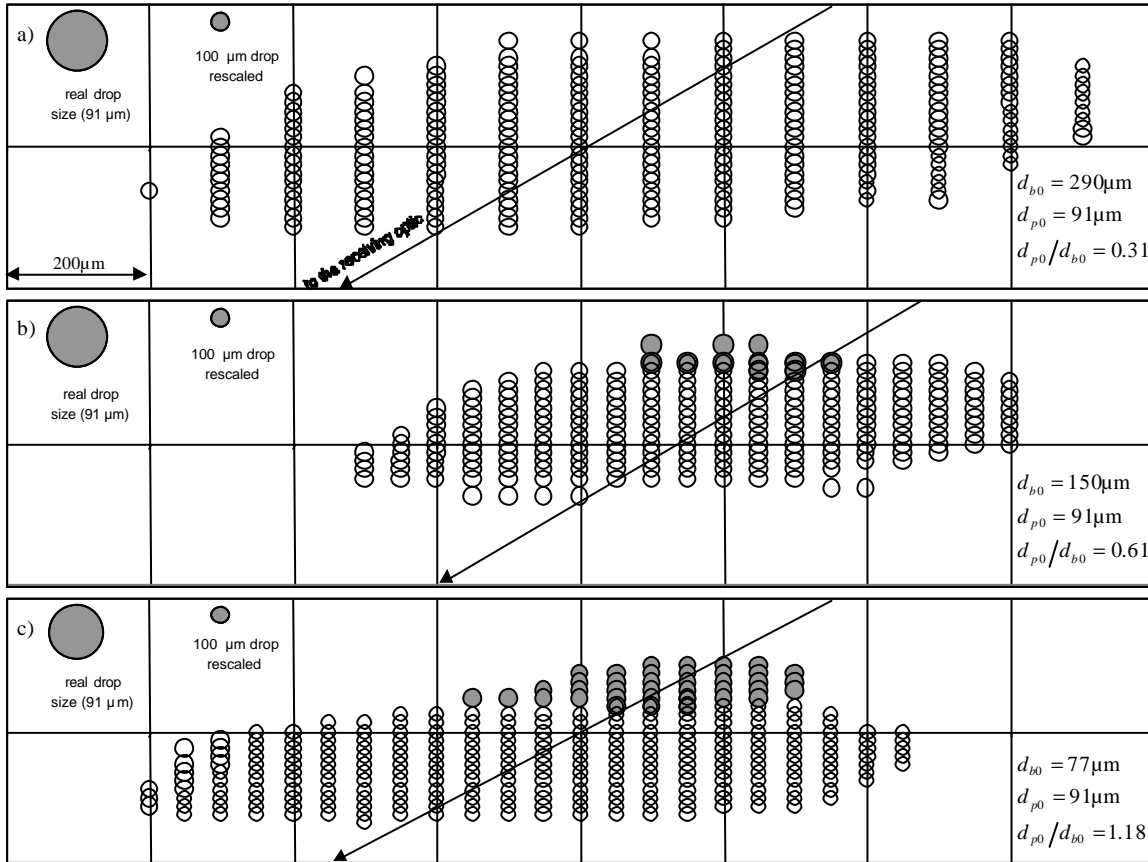


Figure 7: Measurements of monodispersed droplet stream ($d_p = 91 \mu\text{m}$) with different beam waist diameters: a) $290 \mu\text{m}$, b) $150 \mu\text{m}$, c) $77 \mu\text{m}$ ($\varphi_r = 30^\circ$, mask B). The measurements were processed in refraction (?) and reflection (?) mode.

The experimental conditions used for figure 7, given in Table 4, were then used in the theoretical analysis given above. One critical input parameter is the maximum detectable particle diameter d_{p0} . During the measurements the maximum amplitude of the bursts was adjusted using the detector high voltage and the system gain such that the $90\mu\text{m}$ to $100\mu\text{m}$ droplets nearly used the full dynamic range of the processor, without saturation of the electronics. The phase Doppler system has a maximum dynamic range of about 40:1, thus the smallest measurable particle diameter is about $3\mu\text{m}$ to $4\mu\text{m}$, accounting for some deviation from the value given by the manufacturer. This characteristic was checked with a nebuliser, producing droplets in the diameter range up to $4.5\mu\text{m}$. The data rate for such a spray was almost zero with the settings for the monodispersed droplet chain. By increasing the high voltage of the detectors the phase Doppler system was able to detect particles smaller than $4\mu\text{m}$.

Quantity	Symbol	Configuration
Full intersection angle of the laser beams	Θ	$11.1^\circ, 5.72^\circ$
Wavelength	λ	514.5nm
Polarisation angle to beam plane		90°
Beam waist radius	r_m	$77\mu\text{m}, 150\mu\text{m}, 290\mu\text{m}$
Relative refractive index	m	1.334
Reference particle size for ratio determination	d_{p0}	$100\mu\text{m}$
Smallest detectable particle diameter	d_{PL}	$4\mu\text{m}$
Maximum allowable phase difference error	m_V	10°
Maximum phase error per detector	φ_{Err}	5°
Off-axis angle	φ_r	30°
Elevation angle	ψ_r	$< 2.5^\circ$
Dominating scattering order	(d)	Refraction (1)
Unwanted scattering order	(u)	Reflection (0)

Table 4: Example configurations of a phase Doppler system for estimating the error-free measurement range.

In Figure 8 the particle diameter at which a phase difference error of 10° has been computed as a function of detector position, for each of the laser beam waist diameters, $77\mu\text{m}$ (figure 1), $150\mu\text{m}$ and $290\mu\text{m}$, using a smallest detectable particle diameter of $4\mu\text{m}$.

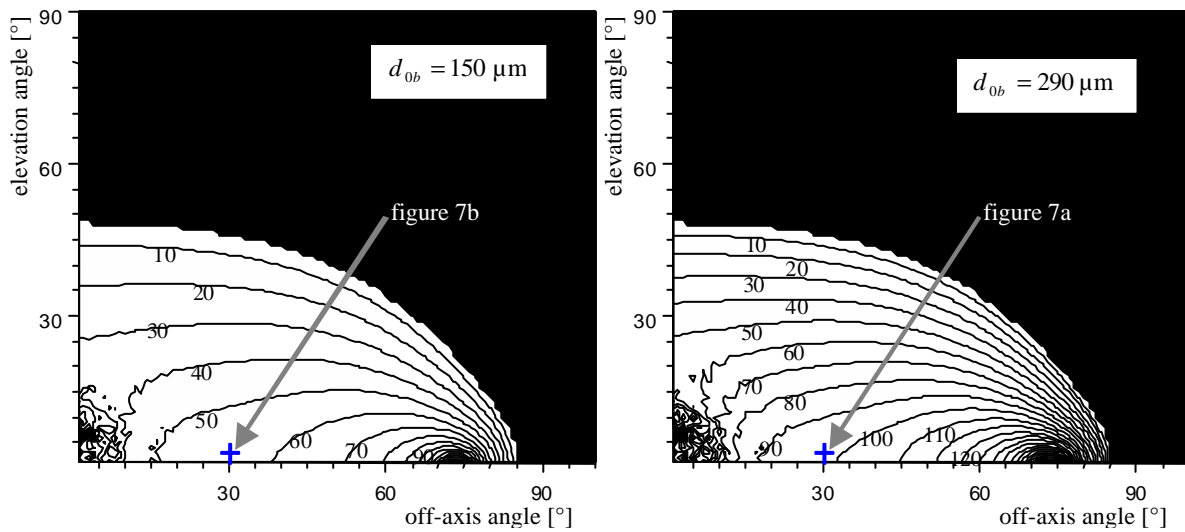


Figure 8: Particle diameter at which a phase difference error of 10° is expected for a laser beam waist diameter of a) $150\mu\text{m}$ and b) $290\mu\text{m}$. For waist diameter of $77\mu\text{m}$ see figure 1.

In the off-axis range of $\varphi_r = 70^\circ \dots 77^\circ$ and the elevation range of $\psi_r = 0^\circ \dots 5^\circ$ first order refraction completely dominates reflection (Brewster angle), thus leading to the maximum measurable particle diameters.

Measurements with the detectors in the black shaded areas are not possible ($M_{crit} < 0.174 = \sin 10^\circ$) since even for plane waves this value of M is not reached.

The optical configurations used to obtain the experimental results in figure 7 have been marked onto the diagrams of figure 1 and figure 8 ($\varphi_r = 30^\circ$, $\psi_r \approx \pm 2.5^\circ$). The predictions in figures 1 and 8 show that the maximum error free particle diameter is $33\mu\text{m}$, $56\mu\text{m}$ and $98\mu\text{m}$ for the beam waist diameters of $77\mu\text{m}$, $150\mu\text{m}$ and $290\mu\text{m}$ respectively. This is in close agreement with the experimental observations in figure 7, where only the $290\mu\text{m}$ diameter volume exhibited error free measurements. If for instance the $150\mu\text{m}$ volume was to be used, the off-axis angle of the receivers would have to be increased to about 70° , as seen from figure 8a.

6. Conclusions

This paper has examined the Gaussian beam effect as a source of error in phase Doppler systems. Specifically the question was asked at what particle diameter do errors begin to occur for a given optical configuration. Rather exact expressions could be derived to answer this question, exemplary applied to the scattering modes reflection and first refraction. Furthermore, direct comparisons between the obtained solutions and well controlled experiments have been made, with excellent agreement. This work therefor reduces for the user the rather complicated theoretical aspects of the Gaussian beam effect to a simple limiting diameter which must not be exceeded.

Acknowledgements

The authors wish to acknowledge financial support from the Deutsche Forschungsgemeinschaft through grant DFG Tr 194/11 and also from the Deutsche Akademische Austauschdienst (DAAD) through the VIGONI program.

References

- [1] van de Hulst H.C. (1981): "Light scattering by small particles", Dover Publications, New York.
- [2] Lock, J.A. (1988): "Cooperative effect among partial waves in Mie scattering", J. Opt. Soc. Am. A **5**, p 2032.
- [3] Hovenac, E. A.; Lock, J. A. (1992): "Assessing the contribution of surface waves and complex rays to far-field Mie scattering by use of the Debye series", J. Opt. Soc. Am. A **9**, pp 781-795.
- [4] Borys, M.; Schelinsky, B.; Albrecht, H.-E.; Krambeer, H. (1998): "Light scattering analysis with methods of geometrical optics for a particle arbitrarily positioned in a laser beam", Optik **108**, p 137.
- [5] Borys, M. (1996): "Analyse des Amplituden- und Phasenverhaltens von Laser-Doppler-Signalen zur Größenbestimmung sphärischer Teilchen", Dissertation, University of Rostock, Germany.
- [6] Gouesbet, G.; Gréhan, G.; Maheu, B. (1985): "Scattering of a Gaussian Beam by a Mie Scatter Center, Using a Bromwich Formalism", J. Opt. Paris **16**(2), pp 83-93. re-published in selected papers on light scattering, SPIE Milestone series, Vol. 951 edited by Kerker, Part I, pp.352-360 (1988).
- [7] Albrecht, H.-E.; Bech, H.; Damaschke, N.; Feleke, M. (1995): "Die Berechnung der Streuintensität eines beliebig im Laserstrahl positionierten Teilchens mit Hilfe der zweidimensionalen Fouriertransformation", Optik **100** pp. 118-124.
- [8] Albrecht, H.-E.; Borys, M.; Damaschke, N.; Tropea, C. (1999): "The imaging properties of particles in laser beams", Meas. Sci. Technol. **10**, pp 564-574.
- [9] Gréhan, G.; Gouesbet, G.; Naqwi, A.; Durst, F. (1991): "Evaluation of Phase Doppler Systems using Generalized Lorenz-Mie Theory", The International Conference on Multiphase Flows '91-Tsukuba, Tsukuba, Japan.

- [10] Gouesbet, G.; Gréhan, G. (1994): "Gaussian Beam Errors in Phase-Doppler Anemometry and their elimination", 7th International Symposium on Application of Laser Techniques to Fluid Mechechnics, Lisbon, Portugal p 1.2.1.
- [11] C. Tropea, T.-H. Xu, F. Onofri, G. Gréhan, and P. Haugen, "Dual mode phase Doppler anemometry," presented at the Seventh International Symposium on Applications of Laser Techniques to Fluid Mechanics, Lisbon, Portugal, 8-11 July 1994.
- [12] Qiu, H.-H.; Hsu, C. T. (1999): "Method of Phase-Doppler Anemometry Free from the Measurement-Volume Effect", *Appl. Optics* **38**, pp 2737-2742.
- [13] Y. Aizu, F. Durst, G. Gréhan, F. Onofri, and T.-H. Xu, "PDA systems without Gaussian beam defects," presented at the Third International Conference on Optical Particle Sizing, Yokohama, Japan, 23-26 August 1993.
- [14] Dantec Measurement Technology A/S (1999): "Particle Dynamics Analyser, Installation & User's guide", Publication no.: 9040U1101, Dantec MT A/S, P.O. Box 121, Tonsbakken 18, DK-2740 Skovlunde, Denmark.